Supplementary material

1. Deriving CO_2 flux budgets for the polar oceans

1.1. Air-ice first-order budget estimation

To establish the budget, we first use measurements from the database to derive average daily CO_2 fluxes for each month for each ocean. These fluxes are then extrapolated to the monthly ice area. Summing those monthly fluxes provides estimates of net CO_2 drawdown into (or release from) the sea ice of the Southern and Arctic Oceans.

In the Arctic, the compiled database and satellite products allow us to distinguish the contributions of first-year ice (FYI), multi-year ice (MYI), and melt ponds (MP). Differentiating between these surface types is essential because they exhibit distinct physical and biogeochemical properties that strongly influence air-ice CO_2 exchange. Under cold conditions, MYI generally has lower permeability and reduced brine volume than the thinner, more saline FYI; however, in summer, FYI can no longer be discriminated from MYI, as surface warming and melting make MYI as permeable as FYI. Therefore, in winter, spring, and fall, we derived monthly FYI fluxes from FYI data, whereas in summer, monthly fluxes are based on measurements from both FYI and MYI. In addition, the summer months include melt pond fluxes, as melt ponds form in late spring and persist through summer, substantially enhancing gas exchange by exposing areas of liquid water on the ice surface.

In contrast, in the Southern Ocean, sea ice is predominantly first-year ice with limited melt pond development. Although features such as polynyas and slush layers over flooded ice can be spatially significant, the compiled database and available satellite products do not allow these to be consistently distinguished. Therefore, monthly fluxes were extrapolated to the total sea-ice area without further subdivision.

Data selection – Panel 1 of Figure S1

In the Arctic, to compute the daily fluxes for FYI during winter months, we excluded fluxes over bare sea ice and frost flowers from our analysis (Figure S1a). In winter, sea ice is nearly always covered by snow, and including fluxes over bare sea ice from which the snow had likely been removed for the measurement would not accurately represent the surface natural state. Frost flower fluxes are also not representative of typical fluxes and are not suited for large-scale extrapolation, given that they are short-lived phenomena of limited spatial extent that occur sporadically under very specific conditions (e.g., thin ice, extreme cold weather; Galley et al., 2015). For the spring and summer months, we included data from snow-covered sea ice and bare sea ice, as snow cover drastically decreases during this period. In the fall, we included both fluxes from snow-covered and bare sea ice, since new ice might not yet have snow on its surface.

In the Southern Ocean, we included only measurements over snow. Slush is spatially relevant in the Southern Ocean, given the extent of flooded sea ice, but most slush flux measurements were obtained after artificially removing snow and deliberately exposing the slush to the atmosphere.

Statistical treatment –Panel 2 of Figure S1

Since flux values do not follow a normal distribution (Shapiro-Wilk test, $p<0.05$), the representative daily CO_2 flux for each month in each ocean is based on the median and interquartile range rather than the mean and standard deviation. Some campaigns deployed autonomous CO_2 chambers capable of producing up to 48 measurements over 25 hours, while others used manual chambers, limiting the number of measurements to 3 per day. To give each survey representing a single location in the ocean the same relative importance and avoid statistical bias, the monthly data were first binned by survey, and monthly median (IQR) fluxes were derived from the binned data (Figure S1 c-g).

In the Arctic, we also derived a representative flux for MYI in winter, fall, and spring. Since the database lacks systematic MYI measurements for each month, it is not possible to derive monthly MYI fluxes. Instead, we compute a single representative daily CO_2 flux based on the median (IQR) of the 40 MYI measurements available throughout the winter (Figure S1b). Similarly, we derived a single representative summer melt pond (MP) flux based on the 25 measurements available in the database (Figure S1b).

Data extrapolation –Panel 3 of Figure S1

In winter, fall and spring, monthly representative fluxes for FYI were extrapolated to the FYI, defined as the total ice area minus the MYI area and representative MYI flux is applied to the monthly MYI area, defined as the ice area in September (Figure S1 h-j, Table S1 and S3). The mean monthly sea-ice area was derived for the years 2000-2023 from EUMETSAT OSI SAF, Global sea ice concentration interim climate data record (SSMIS, v3.0, 2022). In summer, FYI and MYI are no longer distinguished; monthly representative fluxes for ice were extrapolated to what we called summer ice, defined as the total ice area excluding melt pond area (Figure S1h-j, Table S3). Melt pond fluxes were applied to the monthly melt pond area. The mean monthly melt pond area was extracted from the improved Melt Pond Detector 2 (MPD2) Sentinel-3 data for the years 2017 to 2023 (Niehaus et al., 2024). Total air-ice FCO_2 is the sum of the monthly contributions of each ice type (Figure S1k).

For the Southern Ocean, the daily representative fluxes for each month were applied to the sea ice area for that month. Since there were no data for the summer months (February and March), we applied the January fluxes to all summer months. Similarly, there were no data in the winter month of August, so we applied the September fluxes to August.

Finally, the yearly budget is derived by summing the contributions for each month (Figure S1l, Table S1,3).

Table S1. Representative median air-ice FCO_2 fluxes in mmol m^{-2} day^{-1} and spatially extrapolated FCO_2 in Tg C $month^{-1}$ for first-year ice (FYI), summer ice, multi-year ice (MYI) and melt ponds (MP). Total air-ice FCO_2 is the sum of the contributions of each ice type. The numbers in brackets are the first and third quartiles (IQR).

Arctic Ocean		Representative air-ice FCO_2 in **mmol m^{-2} day^{-1}**			Spatially extrapolated FCO_2 in **Tg C $month^{-1}$**			
Ice type	Months	Nbr Field	Nbr data	**Air-ice**	**Air-FYI/Sum. Ice**	**Air-MYI**	**Air-melt pond**	**Total air-ice**
FYI	Jan.	3	22	+0.06 (+0.03, +0.24)	+0.2 (+0.1+0.7)	+0.1 (0.0, +0.1)		+0.3 (+0.1,+0.8)
FYI	Feb.	1	10	+1.42 (+0.88, +1.63)	+4.7 (+2.9,+5.4)	+0.1 (0.0, +0.1)		+4.8 (+2.9,+5.5)
FYI	Mar.	5	198	+0.30 (+0.09,+0.86)	+1.0 (+0.3,+2.9)	+0.1 (0.0, +0.1)		+1.1 (+0.3,+3.0)
FYI	Apr.	4	38	+0.09 (–0.31,+1.27)	+0.3 (–0.1,+4.0)	+0.1 (0.0, +0.1)		+0.4 (–1.0,+4.1)
Summer Ice	May	8	932	0.00 (–0.03,+0.44)	0.0 (–0.1,+1.1)	+0.1 (0.0, +0.1)		+0.1 (–0.1,+1.2)
Summer Ice	Jun.	6	2529	–0.34 (–1.40,+0.49)	–1.1 (–4.4,+1.6)		–0.1 (–0.1,–0.0)	–1.2 (–4.5,+1.6)
Summer Ice	Jul.	1	40	0.00 (0.00,+0.07)	0.0 (–0.2,+0.2)		–0.4 (–0.8,–0.3)	–0.4 (–0.8,–0.1)
Summer Ice	Aug.	2	13	–0.05(–0.35,+0.26)	–0.0 (–0.2,+0.2)		–0.9 (–1.9,–0.6)	–0.9 (–2.1,–0.4)
Summer Ice	Sept.	2	301	–0.83 (–1.75,+0.09)	–1.0 (–2.1,+0.1)		–0.3 (–0.6,–0.2)	–1.3 (–2.7,–0.1)
FYI	Oct.	1	10	+0.17 (+0.17,+0.34)	+0.1 (+0.1,+0.2)	+0.1 (0.0, +0.1)		+0.2 (+0.1,+0.3)
FYI	Nov.	1	20	+0.09 (+0.00,+0.17)	+0.2 (0.0,+0.3)	+0.1 (0.0, +0.1)		+0.3 (0.0,+0.4)
FYI	Dec.	1	4	+0.13 (0.00,+0.25)	+0.32 (0.0,+0.6)	+0.1 (0.0, +0.1)		+0.4 (0.0,+0.7)
MP		3	25	–1.04 (–2.06,–0.69)				
MYI		1	40	+0.10 (0.00,+0.10)				
Total in Tg $year^{-1}$					**+4.7 (–4.4,+17.3)**	**+0.8 (0.00,+0.8)**	**–1.7 (–3.4,–1.1)**	**+3.8 (–7.8, +17.0)**

Southern Ocean					
Total sea ice area	Jan.	1	82	–0.14 (–0.40, –0.01)	–0.2 (–0.5,0.0)
Total sea ice area	Feb.	0	0	na.	–0.1 (–0.3,0.0)*
Total sea ice area	Mar.	0	0	na.	–0.2 (–0.40;0.0)*
Total sea ice area	Apr.	1	8	+0.09(–0.17,+1.17)	+0.2 (–0.3,+2.4)
Total sea ice area	May	1	26	+0.25 (+0.02,+0.88)	+0.8 (+0.1,+2.8)
Total sea ice area	Jun.	2	6	+0.06 (+0.03,+0.10)	+0.3 (+0.1,+0.4)
Total sea ice area	Jul.	1	66	+0.21 (+0.11,+0.35)	+1.1 (+0.6,+1.8)
Total sea ice area	Aug.	0	0	na.	+0.7 (+0.5,+1.7)**
Total sea ice area	Sept.	3	163	+0.13 (+0.10,+0.30)	+0.7 (+0.5,+1.8)
Total sea ice area	Oct.	4	218	–0.04 (–0.09,–0.01)	–0.2 (–0.5, 0.0)
Total sea ice area	Nov.	2	144	–0.13 (–0.25, 0.00)	–0.6 (–1.2,0.0)
Total sea ice area	Dec.	3	211	0.00 (–0.32,+0.01)	0.0 (–0.9,+0.1)
Total in Tg $year^{-1}$					**+2.5 (–2.3,+10.9)**

*computed with CO_2 flux Median (IQR) from January, **computed with CO_2 flux Median (IQR) from September.

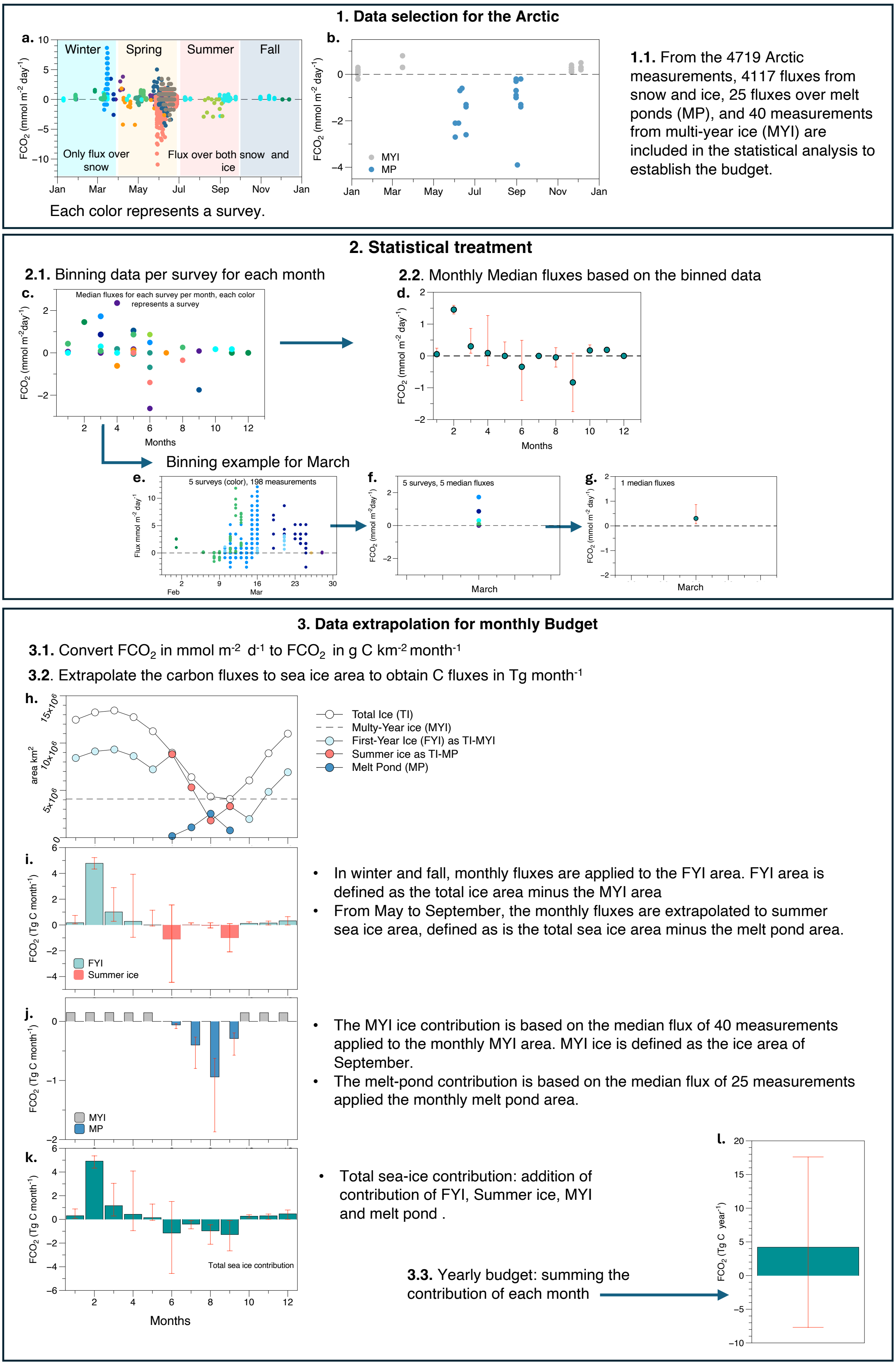

Figure S1. Scheme of the methodology used to establish the monthly and early budget for the Arctic Ocean

1.2. Arctic Ocean air-sea exchange budget

To quantify the seasonal cycle of air–sea CO_2 exchange in the Arctic Ocean, we used monthly climatological fluxes derived from the updated machine-learning pCO_2 product SOM-FFN (Dutch et al., 2025a, 2025b). Air–sea CO_2 fluxes based on the Wanninkhof et al. (2014) gas-exchange parameterisation were extracted for 2000–2016. Monthly means were then derived and aggregated for the RECCAP2 Arctic domain definition (Fay and McKinley, 2014). The resulting climatologies, expressed in both Tg C month^{-1} and mmol m^{-2} day^{-1}, summarize the dominant seasonal patterns of CO_2 uptake and release across the Arctic Ocean (Table S2).

1.3. Southern Ocean air-sea exchange budget

To quantify the seasonal cycle of air–sea CO_2 exchange in the Southern Ocean sea ice zone, we computed monthly climatological fluxes using an ensemble of two widely used observation-based pCO_2 products: CSIR-ML6 (Gregor et al., 2019) and MPI-SOMFNN (Landschützer et al., 2016). Both products used the Wanninkhof et al. (2014) gas-exchange parameterisation and were first regridded and masked according to the RECCAP2 sea ice zone definitions for the Southern Ocean (Hauck et al., 2023). For each product, air–sea CO_2 fluxes were extracted over 2000–2016, and monthly means were then derived and aggregated for the biome. We constructed an ensemble mean by averaging the monthly climatologies from the two pCO_2 products. This ensemble approach provides more stable estimates, particularly for the Southern Ocean, characterised by sparse observations and considerable inter-product uncertainty (Friedlingstein et al., 2025). The resulting climatologies, expressed in both Tg C month^{-1} and mmol m^{-2} day^{-1}, summarize the dominant seasonal patterns of CO_2 uptake and release across the Southern Ocean sea ice zone (Table S2).

Table S2. Monthly air–sea CO_2 fluxes (FCO_2) expressed in mmol m^{-2} day^{-1} and Tg C month^{-1} for the Arctic and Southern Oceans. Fluxes for the Arctic are derived from Dthe Arctic SOMFNN pCO_2 product (Dutch et al., 2025) . Southern Ocean fluxes are computed using an ensemble of the CSIR-ML6 (Gregor et al., 2019) and original MPI-SOMFNN (Landschützer et al., 2016) pCO_2 data products. All values are spatially aggregated according to the RECCAP2 ocean biome definitions for the Arctic and for the sea ice zone (SIZ) of the Southern Ocean (Hauck et al., 2023) for the period 2000–2016.

	Arctic ocean				Southern Ocean SIZ			
	FCO_2 **mmol m^{-2} day^{-1}**		FCO_2 **Tg C month^{-1}**		FCO_2 **mmol m^{-2} day^{-1}**		FCO_2 **Tg C month^{-1}**	
Months	**mean**	**Std**	**mean**	**Std**	**mean**	**Std**	**mean**	**Std**
Jan.	–3.51	4.84	–6.4	1.6	–2.33	0.79	–16.4	6.0
Feb.	–3.02	4.60	–6.5	1.6	–3.19	1.12	–21.9	8.3
Mar.	–1.30	3.22	–5.9	1.2	–2.39	0.98	–16.1	7.2
Apr.	–1.12	2.92	–5.9	1.1	–1.14	0.86	–7.5	6.3
May	–1.27	3.19	–6.7	1.3	0.01	0.56	0.5	4.2
Jun.	–1.54	3.53	–8.1	1.7	0.64	0.43	4.8	3.1
Jul.	–2.11	3.57	–10.4	1.4	1.08	0.33	7.7	2.3
Aug.	–2.44	3.64	–11.3	2.0	1.17	0.37	8.1	2.5
Sept.	–3.28	4.66	–14.9	1.8	0.89	0.35	6.6	2.5
Oct.	–3.85	5.71	–14.1	2.4	0.56	0.27	4.1	2.0
Nov.	–2.67	5.00	–8.6	2.4	–0.03	0.23	–0.3	1.7
Dec.	–3.48	5.09	–7.1	1.6	–1.05	0.42	–7.7	3.2
Total in Tg year^{-1}			**–105.8**	**41.6**			**–38.1**	**16.0**

Table S3. Monthly area used for the extrapolation. The mean monthly total ice area for the Arctic and Southern oceans was derived for the years. 2000-2023 from EUMETSAT OSI SAF, Global sea ice concentration interim climate data record (SSMIS; v3.0, 2022). MYI area is defined as the mean ice area in September. The monthly FYI area is defined as the total ice area minus the MYI area. The mean monthly melt pond area was extracted using the improved Melt Pond Detector 2 (MPD2) Data from Sentinel-3 for the years 2017 to 2023 (Niehaus et al., 2024). The summer ice area is defined as the total ice area excluding the melt pond area.

	Area $10^{-6}km^2$					
	Arctic ocean					Southern Ocean
Months	Total ice	MYI	FYI	MP	Summer ice	Total ice
Jan.	12.47	4.08	8.39			3.46
Feb.	13.24	4.08	9.16			2.15
Mar.	13.44	4.08	9.36			3.03
Apr.	12.74	4.08	8.66			5.74
May	11.25	4.08	7.17			8.88
Jun.	8.98	4.08		0.16	8.82	11.84
Jul.	6.39	4.08		1.08	5.31	14.2
Aug.	4.34	4.08		2.53	1.81	15.69
Sept.	4.08	4.08		0.76	3.32	16.24
Oct.	6.04	4.08	1.96			15.65
Nov.	8.92	4.08	4.84			12.83
Dec.	10.99	4.08	6.91			7.44

References

Dutch, V.R., Bakker, D.C.E., Roobaert, A., Landschützer, P., Roden, N.P., Hoppema, M., Kaiser, J., 2025a. Arctic SOM-FFN Product. https://doi.org/10.5281/zenodo.15056124

Dutch, V.R., Bakker, D.C.E., Roobaert, A., Landschützer, P., Roden, N.P., Hoppema, M., Kaiser, J., 2025b. The Arctic Ocean CO2 Sink: Trends, Uncertainties, and the Impact of Sea Ice. Global Biogeochemical Cycles 39, e2025GB008576. https://doi.org/10.1029/2025GB008576

Fay, A.R., McKinley, G.A., 2014. Global open-ocean biomes: mean and temporal variability. Earth System Science Data 6, 273–284. https://doi.org/10.5194/essd-6-273-2014

Friedlingstein, P., O'Sullivan, M., Jones, M.W., Andrew, R.M., Hauck, J., Landschützer, P., Le Quéré, C., Li, H., Luijkx, I.T., Olsen, A., Peters, G.P., Peters, W., Pongratz, J., Schwingshackl, C., Sitch, S., Canadell, J.G., Ciais, P., Jackson, R.B., Alin, S.R., Arneth, A., Arora, V., Bates, N.R., Becker, M., Bellouin, N., Berghoff, C.F., Bittig, H.C., Bopp, L., Cadule, P., Campbell, K., Chamberlain, M.A., Chandra, N., Chevallier, F., Chini, L.P., Colligan, T., Decayeux, J., Djeutchouang, L.M., Dou, X., Duran Rojas, C., Enyo, K., Evans, W., Fay, A.R., Feely, R.A., Ford, D.J., Foster, A., Gasser, T., Gehlen, M., Gkritzalis, T., Grassi, G., Gregor, L., Gruber, N., Gürses, Ö., Harris, I., Hefner, M., Heinke, J., Hurtt, G.C., Iida, Y., Ilyina, T., Jacobson, A.R., Jain, A.K., Jarníková, T., Jersild, A., Jiang, F., Jin, Z., Kato, E., Keeling, R.F., Klein Goldewijk, K., Knauer, J., Korsbakken, J.I., Lan, X., Lauvset, S.K., Lefèvre, N., Liu, Z., Liu, J., Ma, L., Maksyutov, S., Marland, G., Mayot, N., McGuire, P.C., Metzl, N., Monacci, N.M., Morgan, E.J., Nakaoka, S.-I., Neill, C., Niwa, Y., Nützel, T., Olivier, L., Ono, T., Palmer, P.I., Pierrot, D., Qin, Z., Resplandy, L., Roobaert, A., Rosan, T.M., Rödenbeck, C., Schwinger, J., Smallman, T.L., Smith, S.M., Sospedra-Alfonso, R., Steinhoff, T., Sun, Q., Sutton, A.J., Séférian, R., Takao, S., Tatebe, H., Tian, H., Tilbrook, B., Torres, O., Tourigny, E., Tsujino, H., Tubiello, F., van der Werf, G., Wanninkhof, R., Wang, X., Yang, D., Yang, X., Yu, Z., Yuan, W., Yue, X., Zaehle, S., Zeng, N., Zeng, J., 2025. Global Carbon Budget 2024. Earth System Science Data 17, 965–1039. https://doi.org/10.5194/essd-17-965-2025

Galley, R.J., Else, B.G.T., Geilfus, N., Hare, A.A., Babb, D., Papakyriakou, T., Barber, D.G., Rysgaard, S., 2015. Micrometeorological and Thermal Control of Frost Flower Growth and Decay on Young Sea Ice. Arctic 68, 79. https://doi.org/10.14430/arctic4457

Gregor, L., Lebehot, A.D., Kok, S., Scheel Monteiro, P.M., 2019. A comparative assessment of the uncertainties of global surface ocean CO_2 estimates using a machine-learning ensemble (CSIR-ML6 version 2019a) – have we hit the wall? Geoscientific Model Development 12, 5113–5136. https://doi.org/10.5194/gmd-12-5113-2019

Hauck, J., Gregor, L., Nissen, C., Patara, L., Hague, M., Mongwe, P., Bushinsky, S., Doney, S.C., Gruber, N., Le Quéré, C., Manizza, M., Mazloff, M., Monteiro, P.M.S., Terhaar, J., 2023. The Southern Ocean Carbon Cycle 1985–2018: Mean, Seasonal Cycle, Trends, and Storage. Global Biogeochemical Cycles 37, e2023GB007848. https://doi.org/10.1029/2023GB007848

Landschützer, P., Gruber, N., Bakker, D.C.E., 2016. Decadal variations and trends of the global ocean carbon sink. Global Biogeochemical Cycles 30, 1396–1417. https://doi.org/10.1002/2015gb005359

Niehaus, H., Istomina, L., Nicolaus, M., Tao, R., Malinka, A., Zege, E., Spreen, G., 2024. Melt pond fractions on Arctic summer sea ice retrieved from Sentinel-3 satellite data with a constrained physical forward model. The Cryosphere 18, 933–956. https://doi.org/10.5194/tc-18-933-2024

Wanninkhof, R., 2014. Relationship between wind speed and gas exchange over the ocean revisited. Limnology and Oceanography: Methods 12, 351–362. https://doi.org/10.4319/lom.2014.12.351